

## Lithostratigraphy and metamorphism of the Khudi-Tal area, west central Nepal

Niraj Singh Thakuri<sup>1,3,\*</sup>, Lokendra Pandey<sup>2</sup>, and Lalu Prasad Poudel<sup>3</sup>

<sup>1</sup>Department of Geology, Birendra Multiple Campus, Tribhuvan University, Chitwan, Nepal

<sup>2</sup>Department of Mines and Geology, Kapurdhara Marga-9, Lainchour, Kathmandu, Nepal

<sup>3</sup>Central Department of Geology, Tribhuvan University, Kirtipur, Kathmandu, Nepal

\*Corresponding author's email: niraj.thakuri444@gmail.com

### ABSTRACT

The study is mainly focused on lithostratigraphy, petrography and geological structures to decipher the metamorphic facies and metamorphic history of the Khudi-Tal area along the Marsyangdi Valley, west central Nepal. Geological mapping was carried out covering 142 sq. km, on the scale of 1:50000. The Main Central Thrust (MCT) separates lithological succession of the Lesser Himalaya and Higher Himalaya around Bahundanda, Probhi and Naiche of the Khudi-Tal area. Lithological succession is dominated by metapelitic to psammatic schist, siliceous to dolomitic marble, quartzites, graphitic to garnet schist, kyanite garnet gneiss and banded gneiss from south to north. The kyanite isograd follow the MCT separating Kyanite zone with mineral assemblages Ky+Grt+Qtz+Ms+Bt+Pl of the Higher Himalaya and Garnet zone as Grt+Bt+Ms+Chl+K-Fel+Pl+Qtz in pelitic rocks, Bt+Ms+Chl+Plag+Qtz in psammatic rocks and Cal/Dol+Qtz+Pl+Bt+Ms in calcareous rock of the Lesser Himalaya. Based on the mineral assemblages, the Higher Himalaya belongs to Amphibolite Facies whereas the Lesser Himalaya belongs to Epidote-Amphibolite Facies. The lithological succession of the Higher and the Lesser Himalaya has undergone poly-phase metamorphism. In the Lesser Himalayan zone rocks, the regional burial metamorphism  $M_1$  (pre-MCT/ eo-Himalayan) is followed by barrovian type garnet grade inverted metamorphism  $M_2$  and later post-MCT retrogressive metamorphism  $M_3$ . In the Higher Himalaya rocks, the early phase kyanite bearing medium temperature/ high pressure regional prograde metamorphism  $M_1$  (pre-MCT/ eo-Himalayan) is followed by barrovian type inverted metamorphism  $M_2$  (syn-MCT/ neo-Himalayan) and over printed by later phase retrogressive metamorphism  $M_3$  (post-MCT).

**Keywords:** Lithostratigraphy, MCT, poly-phase metamorphism, Khudi-Tal area, west-central Nepal

**Received:** 21 April 2022

**Accepted:** 30 July 2022

### INTRODUCTION

During early Tertiary, the continental collision between the Indian and Eurasian plates results the formation of the Himalaya by N-S compression, forming various geological structures like thrusts and strike slip and normal fault system (Gansser, 1964; Molnar and Tapponnier, 1975; Tapponier et al., 1986; Valdiya, 1980). These faults are termed as the South Tibetan Detachment Fault System (STDS), Main Central Thrust (MCT), Main Boundary Thrust (MBT) and Himalayan Frontal Thrust (HFT) from north to south respectively. These faults divided the overall Himalaya in to four tectonic divisions as the Tibetan Tethys, Higher Himalaya, Lesser Himalaya and Sub Himalaya (Siwalik) respectively (Gansser, 1964).

The research in the Lesser and Higher Himalaya are mainly focused in geological evolution, tectonics, petrography, micro-tectonics, metamorphism, structural studies and geochronology (Gansser, 1964; Le Fort, 1975; Pêcher, 1977; Stöcklin and Bhattarai, 1977; Colchen et al., 1986, 1980; Stöcklin, 1980; Arita, 1983; Hodges et al., 1988, 1996; Harrison et al., 1997; Paudel and Arita, 2000; Catlos et al., 2001; Avouac, 2003; Gehrels et al., 2003; Martin et al., 2005;

Pearson and DeCelles, 2005; Wobus et al., 2005; Bollinger et al., 2006; Kohn, 2008; Searle et al., 2008; Corrie and Kohn, 2011; Paudyal and Paudel, 2011; Nadin and Martin, 2012; Khanal and Robinson, 2013; Godard et al., 2014; Dhital, 2015). The Higher Himalaya of Western Nepal consists of Mesoproterozoic to Early Palaeozoic medium to high-grade metasedimentary rocks and crustal melts (Parrish and Hodges, 1996). The Higher Himalaya is bounded by brittle-ductile shear zone as MCT Zone to the south (Arita, 1983) and the South Tibetan Detachment System on the north (Le Fort, 1975; Searle et al., 2008; Searle, 2010). The brittle-ductile shear zone is considered equivalent to Nawakot Complex of the Lesser Himalaya (Stöcklin, 1980) It is characterized by metapelites, massive quartzites, marbles, metacarbonates and schists followed by kyanite to sillimanite-grade schists, paragneisses and migmatites in upper section (Colchen et al., 1986; Hodges et al., 1996; Larson and Godin, 2009; Le Fort, 1975). To the south, the Lesser Himalaya consists of low to medium grade metasedimentary and metavolcanic rocks of Mesoproterozoic (?) to lower Eocene age (Parrish and Hodges, 1995; Stocklin, 1980). It is overlain by Late Palaeozoic and Early Tertiary sediments of the Gondwana sequences (Sakai, 1983) and high-

grade rocks of the Higher Himalaya overthrust along the MCT, resulting a thick ductile shear zone (MCT zone) at 22±20 Ma (Schelling and Arita, 1991; Hubbard and Harrison, 1989). The Higher Himalaya and Lesser Himalaya of the central Nepal has undergone polyphase of metamorphism (Le Fort, 1975; Arita, 1983; 1992; Hodges et al., 1994; Paudel, 2000). Accordingly, in the Lesser and Higher Himalaya of central Nepal, multistage of the metamorphic events, petrography, metamorphic facies and zonation have been reported from Kaligandaki Khola, Modi Khola and Darondi River (Hodges et al., 1988; Le Fort, 1996; Rai et al., 2005; Vanney and Hodges, 1996, Paudel and Arita, 2000). They have also reported the numerous of deformation phases, caused during episodes of metamorphic events in different time. Also, they mentioned events of metamorphism as the earlier high T/ high P kyanite

grade Barrovian type metamorphism (Eo-Himalayan) followed by lower P/ high sillimanite grade metamorphism (Neo-Himalayan) in the Higher Himalaya and burial type prograde regional metamorphism (Eo-Himalayan) followed by garnet grade inverted metamorphism (Neo-Himalayan) in the Lesser Himalaya which in turn are over overprinted by the retrograde phase metamorphism. However, most of the rock succession of the Lesser Himalaya and the Higher Himalaya are mapped and studied in the regional scale (Parson et al., 2016; Searle and Godin, 2003). The present study focuses on lithostratigraphy based geological mapping, petrography, location of the MCT separating the two zones, and metamorphism of the rock succession of the Lesser and Higher Himalaya of the Khudi-Tal area along Marsyangdi Valley (Fig. 1).

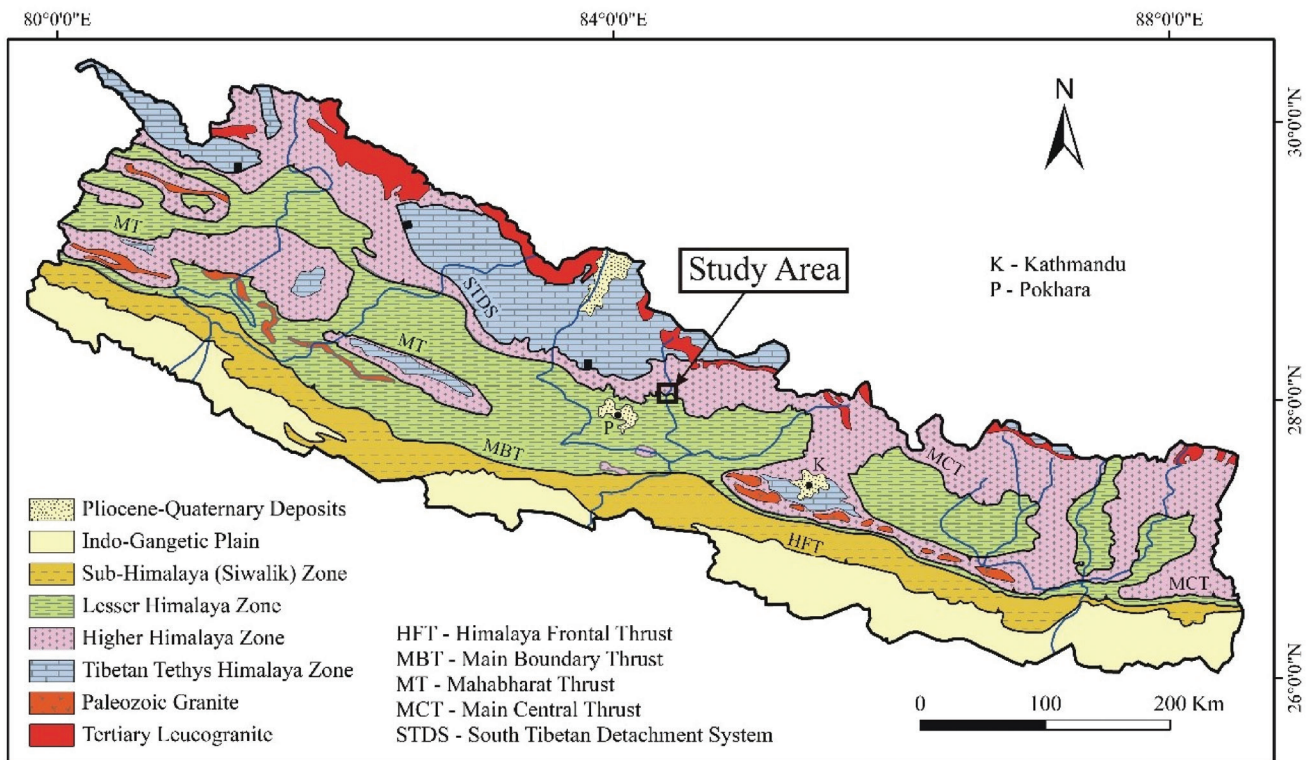


Fig. 1: Geological map of Nepal showing location of the study area (modified after Amatya and Jnawali, 1994).

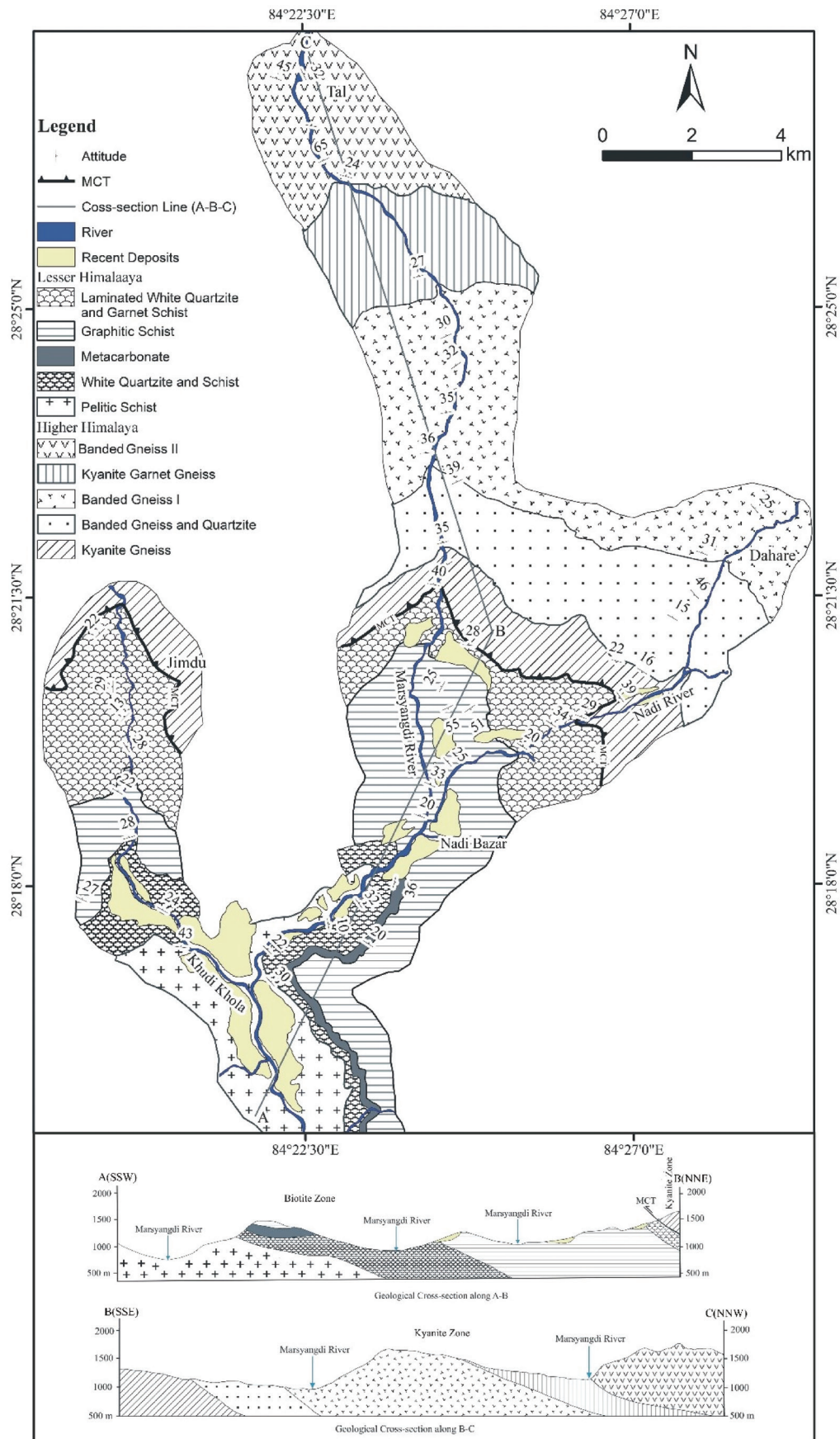
**METHODOLOGY**

In this research, the topographic map of Bahundanda (sheet No. 2884 10) was used as base map, published by Department of Survey, Government of Nepal 1998 on scale of 1:50,000. In field, all the mappable lithological units were mapped with their attitudes and observed in detail concerning geological structures, metamorphism and mineral resources from all possible routes like road section, foot trail and valley. The final geological map was prepared with the stratigraphy following the international stratigraphic code. 45 thin sections were prepared from oriented representative samples taken during the traverse in field for the petrographic analysis in laboratory of the Central Department of Geology, Tribhuvan University.

Geological map, geological cross section, isograd map and generalized columnar section were prepared with help of ArcGIS 10.5 (student version) and Corel Draw X7.

**LITHOSTRATIGRAPHY**

In this study, litho-units of the Lesser Himalaya and Higher Himalaya along the Marsyangdi Khola are classified following the lithostratigraphy of Colchen et al., (1980) and Stöcklin and Bhattarai (1980) which are further classified into different distinct mappable litho type. Lithostratigraphically, the Khudi-Tal area has been divided into two lithological successions as the Higher Himalaya and the Lesser Himalaya, separated by the Main Central Thrust (Figs. 2, 3).



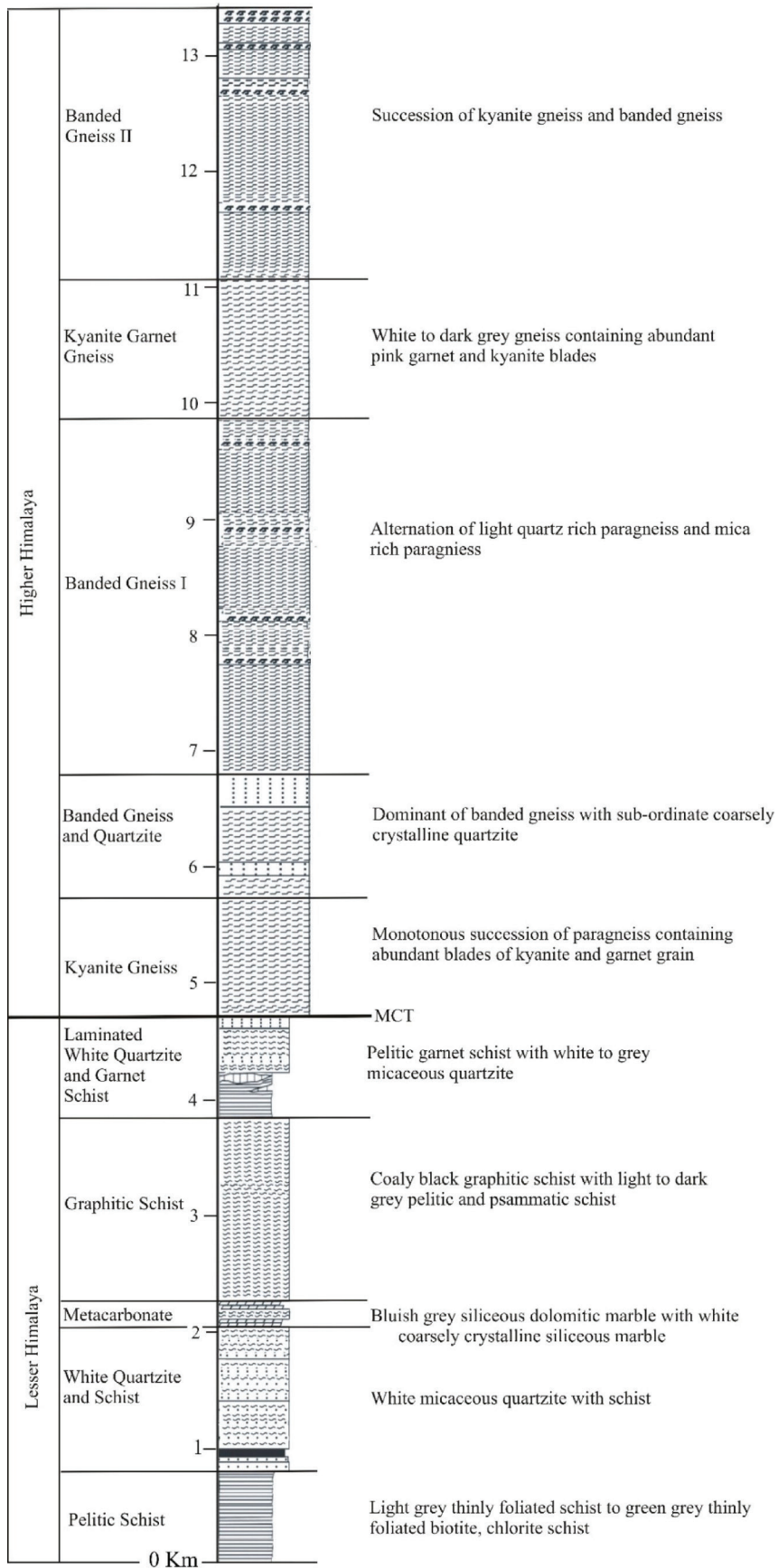


Fig. 3: Generalized columnar section of the study area. MCT: Main Central Thrust.

## **Lesser Himalaya**

### ***Pelitic Schist***

Pelitic Schist is well exposed around Simalchaur, Bandre and Latephat area (Fig. 2). It is the lowermost unit in present study that comprises the light grey, fine to medium grained, thinly foliated phyllite to greenish grey biotite chlorite schist with occasional occurrence of garnet (Fig. 4a). The well-developed lineation is defined by the preferred alignment of biotite grains that trends towards NNE to SSW direction. It is overlain by the micaceous quartzite of White Quartzite and Schist with the gradational contact.

### ***White Quartzite and Schist***

It is well exposed in west of Pallotari, Bhulbhule, Nandeswora and western part of Tarache village (Fig. 2). It is characterized by thick bands (50m) of white, thin to medium bedded, medium grained micaceous quartzite at the bottom, followed by alteration of white to bluish grey, thin to thickly bedded (2 mm to 32 mm), fine to medium grey quartzite, light grey, thinly foliated, medium grained pelitic schist and dark green, massive (100 m thick), strongly foliated, medium to coarse grained amphibolite to actinolite-tremolite schist. The mineral composition of this formation is represented by quartz, feldspar, hornblende, actinolite, biotite and muscovite. The dolomitic marble of Metacarbonates transitionally overlies the rock sequences of White Quartzite and Schist.

### ***Metacarbonates***

It is well exposed around Bhulbhule, Bhumse and Thranche area. However, it completely disappears along Khudi Khola section (Fig. 2). It comprises the bluish grey, thick bedded to massive, siliceous nature, medium to coarse grained dolomitic marble with thin bands of white, coarsely crystalline siliceous marble. The rocks of the Metacarbonates are overlain by the rocks of the Graphitic Schist without distinct geological boundary as it is covered with the recent deposit.

### ***Graphitic Schist***

It is exposed in Bhumse, Rintan, NadiBajar in the eastern part, Chhaharekhola and Ghimrun, Goptegaun and Sobje village. It comprises the dark grey colored, slightly weathered slate, fine grained, thick succession (> 150 m) of coaly black phyllite with slaty cleavage in the left bank of the Chhaharekhola, light grey phyllite and calcareous horizon with medium grained schist in the upper part of the succession. It gradually passes into the rock sequences of White Quartzite and Garnet schist with sheared exposures.

### ***White Quartzite and Garnet Schist***

It is exposed around Nagdi Khola, Khudi Khola, Sabje village area. It overlies the calcareous horizon bed of Graphitic Schist with highly sheared zone. It is characterized by thin inter banding of medium grained pelitic schist and medium grained micaceous white quartzites. The garnet (upto 1.2 cm) is common in pelitic schist at the lower part however the upper

part consists of thickly foliated, highly deformed garnet schist with rare intercalation of grey quartzite. It is the uppermost section of the rock sequences of Lesser Himalaya along which the rock sequences of the Higher Himalaya are thrust through the MCT.

## ***Higher Himalaya Zone***

In the present study, the Higher Himalaya is characterized by five lithological units as Kyanite Gneiss, Banded Gneiss and Quartzite, Banded Gneiss I, Kyanite-Garnet Gneiss and Banded Gneiss II, based on distinct litho-type and mineral association from lower section to upper section respectively.

### ***Kyanite Gneiss***

It is the lowermost litho-unit of the Higher Himalaya in the Marsyangdi Khola section and well exposed around Bahundanda, Lillibhir, Badalbidaune and Naiche area (Fig. 2). It comprises the monotonous succession of light grey, coarse to very coarse grained, thickly bedded paragneiss with abundant of kyanite blades and garnet. The major mineralogical compositions of this unit are muscovite, biotite, quartz, garnet and kyanite. The garnet is reddish brown in color with size range from mm to 8 mm. The light to dark blue, kyanites (1.5 to 3 cm, along long axis) are fractured, bent, lineated and oriented along the foliation. The total thickness of this unit is 1015 m.

### ***Banded Gneiss and Quartzite***

This unit is well exposed around Ghermu village, Marsyangdi valley and Nagdi valley (Fig. 2). It conformably overlies the Kyanite Gneiss by the dominance of light-colored banded gneiss with few proportions of coarsely crystalline quartzite beds (Fig. 3). The unit is characterized by the garnet (up to 0.4 mm) bearing light grey colored, coarse grained paragneiss at its lower part whereas dark colored, thin to thick bedded, muscovite-biotite rich gneiss with segregated quartz lenses and grey colored, coarsely crystalline, micaceous quartzite in its upper part. The major mineralogical compositions of the unit are garnet, muscovite, biotite, quartz and feldspar. The mica size (0 to 8 mm) increases from lower to upper part of the succession. The thickness of this unit is 1062 m.

### ***Banded Gneiss I***

It is well exposed around Syage, Shreechau, Jittal and Dahare area. It overlies the Banded Gneiss and Quartzite through gradual contact and comprises the alternation of light grey colored, medium to coarse grained, quartz rich paragneiss and dark grey colored, muscovite-biotite rich paragneiss, forming typical banding. The thickness of the quartz band ranges from 1 mm to 1.4 cm. The banded gneiss consists of distinct thin bands of leucocratic and melanocratic layers. The major mineral compositions of this unit are muscovite, biotite, plagioclase and quartz. The augen texture are developed due to quartz segregations, ranges from mm to 22 cm. Characteristics folded quartz veins, boudins and quartz pods are common in banded gneiss. The total thickness of this unit is 1025 m.

### **Kyanite-Garnet Gneiss**

Kyanite-Garnet Gneiss is well exposed around Puranojagat, Jagat and Chyameche village area. It overlies the Banded Gneiss I with gradual contact and marked by the appearance of kyanite and pink colored garnet in augen gneiss. It consists of alternation of quartz-feldspar rich gneiss and biotite rich dark coarse grained, grey gneiss with abundance of pink garnet (upto 1.2 cm) and kyanite blades (2.2 to 2.5 cm, along long axis). The light to dark blue kyanites shows the lineated fabric and are oriented along the foliation. The major mineral compositions of this unit are kyanite, garnet, muscovite, biotite, plagioclase and quartz. This unit passes to the Banded Gneiss II through gradual contact.

### **Banded Gneiss II**

Banded Gneiss II is well exposed in Pune, Sattle, Gheran and Tal village area along the Marsyangdi valley. It is uppermost part of the study area and characterized by kyanite gneiss and light colored dominated banded gneiss. The major mineral composition is represented by kyanite, garnet, feldspar, muscovite and quartz. The total thickness of this unit is 2370 m in the study area.

## **PETROGRAPHY**

The thin sections of the oriented representative sample from all the litho-type of study area were prepared for petrographic study. This study is mainly focused on mineral paragenesis, mineral fabric, mineral assemblages and micro structures. The petrographic characteristics of the representative samples are described below. The mineral abbreviations are after Kretz (1983).

### **Petrographic study from Lesser Himalaya samples**

#### ***Pelitic Schist***

*Sample No. ML5:* The sample represents the green grey, thinly foliated, biotite-chlorite schist. Its mineral assemblage under the petrological microscope is Grt+Bt+Ms+Cl+Pl+Qtz. The overall modal composition of the sample is 24% Qtz, 6% Pl, 34% Ms, 24% Bt, 8% Cl and others. The quartz grains are subhedral to anhedral and mica minerals are elongated. The one set of foliations is defined by the elongated mica minerals and recrystallized equant quartz minerals (Fig. 4a).

#### ***White Quartzite and Schist***

*Sample No. 5T3:* The sample represents the thinly banded micaceous quartzite (Fig. 4b). The mineral assemblages are Ms+Bt+Qtz. The overall modal composition is estimated as 81% Qtz, 11% Bt, 8% Ms, 2% opaque. The quartz size varies from 0.2 mm to 0.5 mm and biotite is up to 0.5 mm. The quartz grain shows the undulatory extinction and triple grain boundary junction indicating nearly equilibrium growth. The orientation of elongated platy minerals shows one set of foliations.

*Sample No. 5T1:* The sample represents the actinolite schist (Fig. 4c). The mineral assemblage of this sample is Hbl+Tr+Act+Pl+Qtz. The overall modal composition is 40%

Hbl, 18% Act, 20% Tr, 14 % Qtz and 6% Pl and others (Fig. 4c). The sizes of the mineral grains are from medium to fine grain as 0.02 to 0.44 Qtz and 0.01 mm to 1.25 Tr. The foliation is defined by the parallel alignment of the minerals including hornblende and tremolite indicating nematoblastic texture. The hornblende mineral shows strongly green pleochroism and an actinolite mineral has light green to yellow.

#### ***Metacarbonates***

*Sample No. 6T3:* The sample represents the siliceous dolomite (Fig. 4d). The mineral assemblages is Cal/Dol+Qtz+Pl+Bt+Ms. The modal composition of the sample is 80% Dol/Cal, 6% Qtz, 5% Ms, 3% Bt, 12% Pl. The shape of the grain size of the dolomite is subhedral to anhedral and feldspar is anhedral (Fig. 4d).

#### ***Graphitic Schist***

*Sample No. 4T9:* The sample represents the dark grey to black calcareous schist (Fig. 4e). The mineral assemblages are Grt+Ms+Bt+Cal+Qtz. The overall modal composition is 30% Qtz, 35% mica, 35% calcite (Fig. 4e). The sample shows the porphyroblast of garnet with the spiral inclusion of quartz and calcite at lower left edge. The shape of the garnet is euhedral to anhedral. The foliation is defined by the elongated mica minerals.

#### ***Laminated White Quartzite and Garnet Schist***

*Sample No. 3T1:* The sample represents the sample of micaceous quartzite (Fig. 4f). The mineral assemblage present is biotite-muscovite-quartz. The modal compositions of minerals are 83% Qtz, 7% Bt, 8% Ms and 2% voids. The size of quartz grain ranges from 0.2 mm to 0.5 mm and biotite are up to 0.24 mm (Fig. 4f). The one set of foliations is defined by the oriented mica and elongated quartz.

### **Petrographic study from the Higher Himalaya Zone samples**

#### ***Kyanite Gneiss***

*Sample No. GM10:* The sample represents the kyanite gneiss (Fig. 5a). The mineral assemblages are Ky+ Ms+Bt+Qtz+Kfs. The overall modal composition is 36% Qtz, 10 % Kfs, 27% Bt, 13% Ms, 6% Ky, 10% others (Fig. 5a). The kyanite size ranges from 0.25 mm to 1.98 mm and mica size ranges from 0.15 mm to 0.66 mm (along long axis). The zoned kyanite is observed. The inclusion of mica is present in kyanite. The shape of the kyanite is bladed, quartz mineral is sub-hedral to anhedral and mica is platy.

#### ***Banded Gneiss and Quartzite***

*Sample No. GM13:* The sample represents the banded gneiss (Fig. 5b). The mineral assemblages are Ms+Bt+Pl+Or+Qtz. The overall modal composition is 35% Qtz, 5% Or, 10% Pl, 30% Bt, 14% Ms, 6% Cl (Fig. 5b). The size of the minerals grain ranges from 0.17 mm to 1.2 mm Bt, 0.07 mm to 12 mm Qtz and 0.11 mm to 0.49 mm Ms. The undulatory extinction in the quartz with biotite inclusion is observed. The zoning in the biotite is seen.

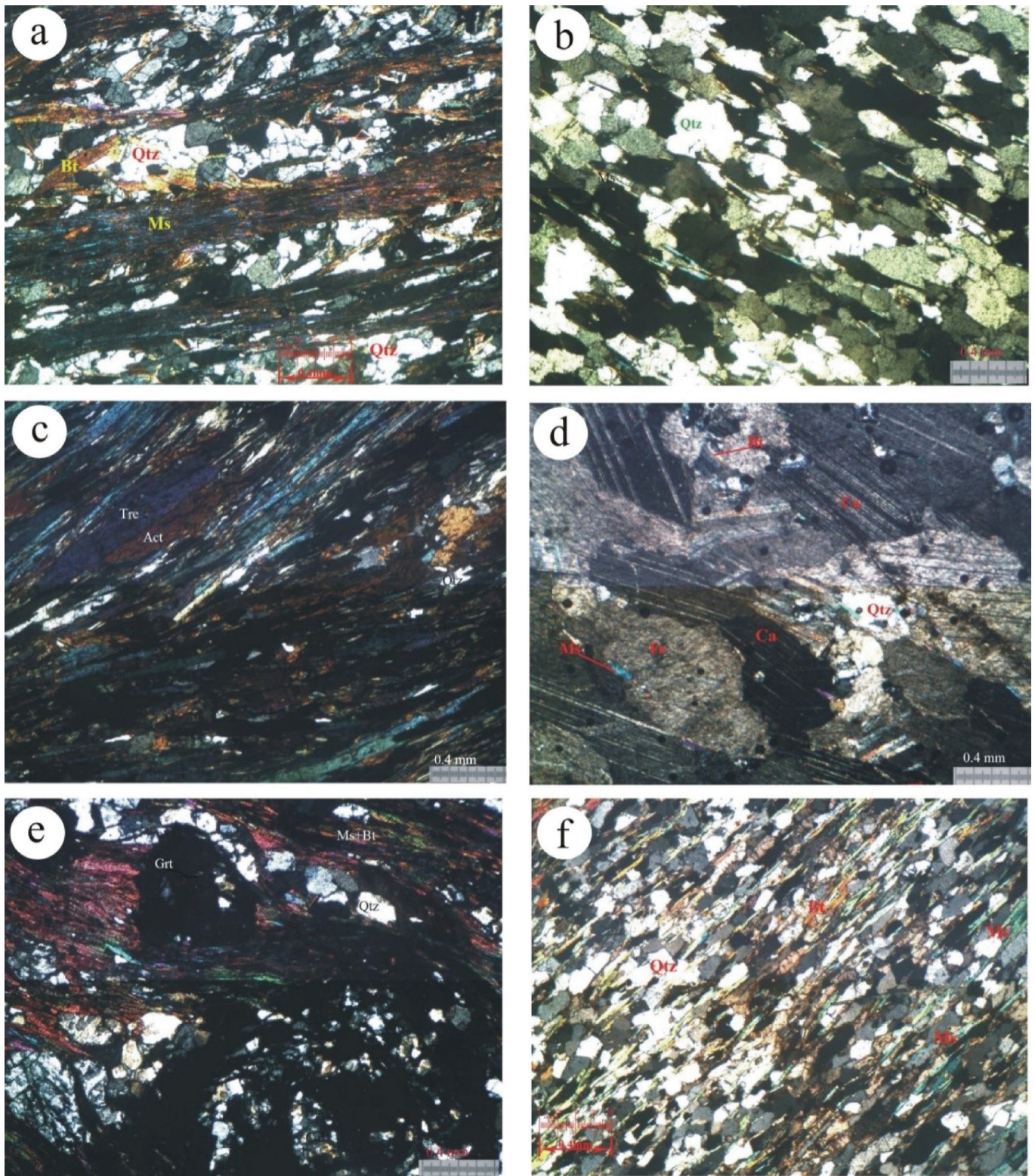
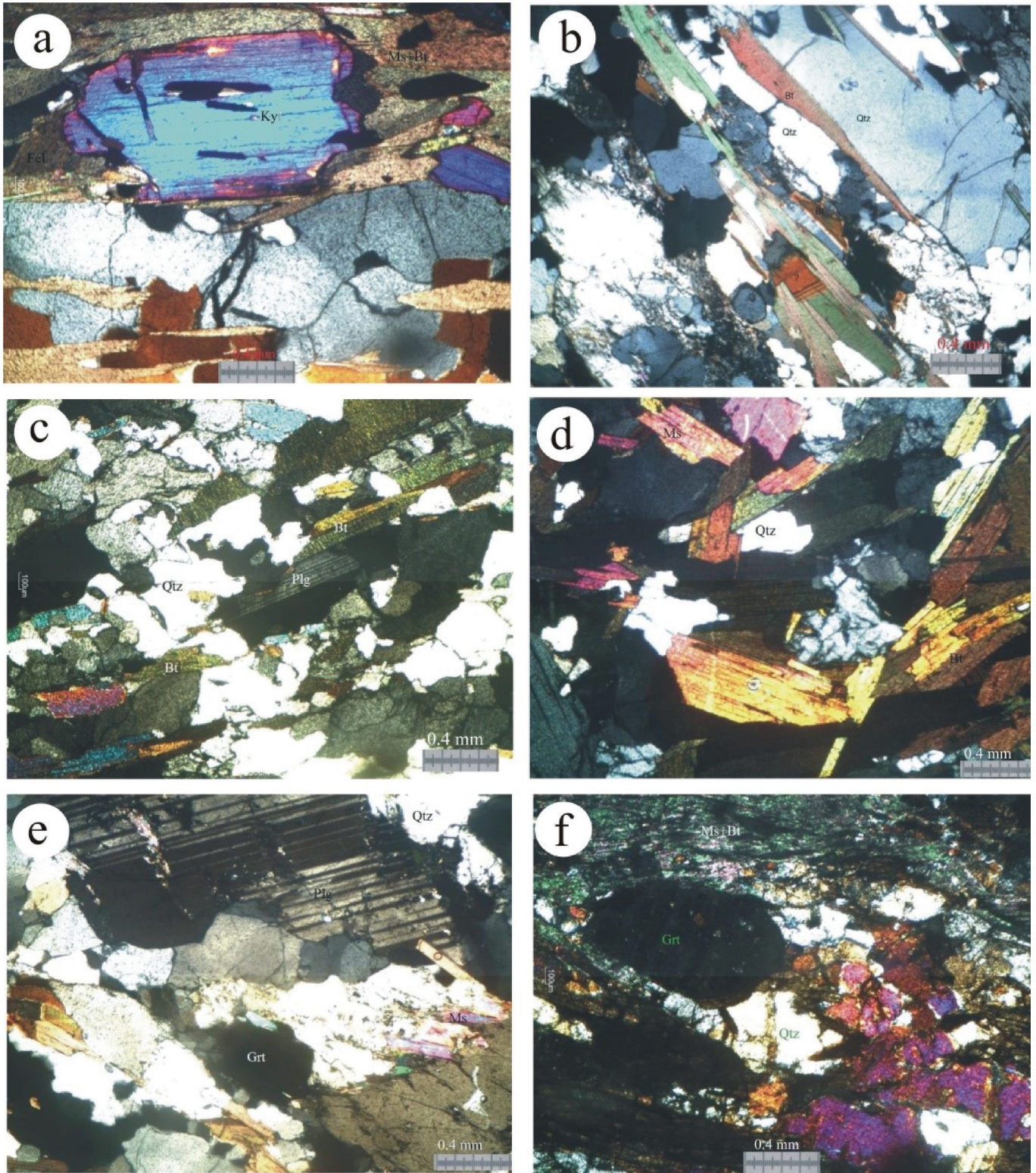


Fig. 4: (a) Photomicrograph showing the interlayering of mica and quartz in pelitic schist (Sample No. ML5), (b) Photomicrograph showing nearly equigranular quartz grains in micaceous quartzites (Sample No. 5T3), (c) Photomicrograph showing neunematoblastic texture in actinolite schist (Sample No. 5T1), (d) Microphotograph showing twinning in calcite minerals in dolomite (Sample No. 6T3), (e) Photomicrograph showing the porphyroblast of garnet with quartz inclusion (Sample No. 4T9), (f) Photomicrograph showing mica in the white laminated quartzite (Sample No. 3T1). Abbreviations of minerals in alphabetic orders: Act: Actinolite, Bt: Biotite, Cl: Chlorite, Dol: Dolomite, Grt: Garnet, Hbl: Hornblende, Ky: Kyanite, Or: Orthoclase, Tre: Tremolite.



**Fig. 5:** (a) Photomicrograph showing the zoned kyanite with the inclusion of mica minerals (Sample No. GM10), (b) Photomicrograph showing the preferred orientation of mica minerals in banded gneiss (Sample No. GM13), (c) Photomicrograph showing polysynthetic twinning of plagioclase in gneiss (Sample No. GM17), (d) Photomicrograph showing the 3-set of orientation of mica minerals and segregated quartz grain in gneiss (Sample No. GM19), (e) Photomicrograph showing the polysynthetic twinning plagioclase and garnet in Kyanite garnet gneiss (Sample No. GM24), (f) Photomicrograph showing the alteration of garnet into biotite along the rims of garnet grain in gneiss (Sample No. GM31). Abbreviations of minerals in alphabetic orders: Act: Actinolite, Bt: Biotite, Cl: Chlorite, Dol: Dolomite, Grt: Garnet, Hbl: Hornblende, Ky: Kyanite, Or: Orthoclase, Tre: Tremolite.



**Banded Gneiss I**

*Sample No. GM17:* The sample represents the gneiss (Fig. 5c). The mineral assemblages are Ms+Bt+Pl+Qtz. The overall modal composition is 37% Qtz, 30% Pl, 20% Bt, 13% Ms. The size of the minerals grain ranges from 0.51 mm Pl, 0.74 mm to 0.99 mm Qtz, 0.46 mm to 0.15 mm mica. The shape of the quartz is sub-hedral to euhedral and mica is platy. The pressure solution shows the indented contact between the adjacent grains in thin section. The plagioclase shows the polysynthetic twinning.

*Sample No. GM19:* The sample represents the gneiss with segregation of quartz (Fig. 5d). The mineral assemblage in the thin section is Ms+Bt+Qtz+Fel. The overall modal composition is 35% Qtz, 30% Bt, 15% Fel, 20% Ms. (Fig. 5d). The mineral grain size is Ms 0.4 mm, Qtz 0.39 mm, Bt 0.9 mm (long axis) and 0.19 mm (short axis). The shape of quartz is sub-hedral to anhedral. The three set of foliations is defined by the cross-cutting relation of elongated muscovite at top left of the thin section.

**Kyanite-Garnet Gneiss**

*Sample No. GM24:* The representative sample is of kyanite gneiss (Fig. 5e). The mineral assemblage is defined as Ky+Grt+Ms+Bt+Pl+Qtz. The modal composition of sample is 34% Qtz, 20% mica, 46% Fel and others. The general shape of the quartz is sub-hedral to anhedral, garnet is sub hedral and mica is platy. Plagioclase shows polysynthetic twinning (Fig. 5e).

**Banded Gneiss II**

*Sample No. GM31:* The representative sample consists of banded gneiss (Fig. 5f). The mineral assemblages of Ky+Grt+Pl+Or+Ms+Bt+Qtz. The overall modal composition is 60% Qtz, 33% mica, 15% Fel, 2% others (Fig. 5f). Mostly, the grain shape of the minerals is anhedral (quartz) to elongated (mica) and the garnet shape is sub-hedral. In the thin section, the garnet grain with top south sense of shear is observed. The inclusion of biotite is seen in garnet. And the alteration of garnet to the biotite can be seen along the rims of the garnet. The size of the garnet range upto 0.72 mm, quartz is 0.48 mm to 0.03 mm and mica is 0.14 mm to 0.01 mm.

**METAMORPHISM****Metamorphic zonation**

Two metamorphic zones as garnet zone in the south and kyanite zone in the north separated kyanite isograd have been identified based on the index mineral observed in field and petrography of representative samples (Fig. 2). The kyanite isograd is marked with the presence of kyanite as index minerals around Bahundanda and Naiche village. However, it coincides with MCT, separating kyanite zone from underlying garnet zone. Kyanite zone covers the litho-units of the Higher Himalaya as kyanite garnet gneiss to banded gneiss (Fig. 2, Table 1). It is well observed in gneiss to banded gneiss of the Higher Himalaya. The size of the kyanite ranges from 1.5 cm to 3 cm

and well observed in hand sample and thin section (Fig. 5a).

Accordingly, the intensity of grade increases from garnet grade in south to kyanite grade to north. The garnet isograd lies around the Besisahar and Duwar of Lamjung District (Pokhrel, 2015). In present study, the garnet zone is exposed around Sera village to the north upto Probi, Jimdu, Ghoptegaun and south of Bahundanda (Fig. 2). It consists of lithological units of the Lesser Himalaya as metapelitic to psammitic schist, siliceous to dolomitic marble, quartzite, graphitic to garnet schist (Table 2). The garnet is well observed in pelitic and psammitic rocks in both hand sample and thin section (Fig. 4). The size of the garnet ranges from 0.4 cm to 1.2 cm in garnetiferous schist.

**Metamorphic facies**

Based on the mineral zonation and mineral assemblages, the study area belongs to two metamorphic facies as garnet grade epidote-amphibolite facies of the Lesser Himalaya to kyanite grade amphibolite facies of the Higher Himalaya (Ehlers and Blatt, 1999; Table 1). The mineral assemblage of epidote-amphibolite facies is characterized by Grt+Bt+Ms+Chl+Kfs+Pl+Qtz in pelitic rocks, Bt+Ms+Chl+Pl+Qtz in Psammitic rocks and Cal/Dol+Qtz+Pl+Bt+Ms in calcareous rock. Amphibolite facies in pelitic rock is marked by the development of mineral assemblage Ky+Grt+Bt+Qtz and Ky+Grt+Ms+Bt+Pl in psammitic rocks (Table 1).

**Poly-phase metamorphism**

Based on various geological structures and deformation observed in field and petrography, the study area has undergone polyphase of metamorphism. Three metamorphic events have been observed in the Higher Himalaya. The kyanite and garnet rich litho-units suffered high Pressure/ low temperature amphibolite facies Barrovian type prograde metamorphism (eo-Himalayan/ pre-MCT) was the first event of metamorphism  $M_1$  (Fig. 5a). The second event of metamorphism  $M_2$  (neo-Himalayan/ syn-MCT) was evidenced by the spiral quartz inclusion within the garnet (Fig. 4f), top to south sense of indicator in asymmetric boudin (Fig. 5a) and NNE sense of sharing indicated by the lineated kyanite and mica minerals. It is due to the shearing and thrusting along the MCT during upliftment (Stäubli, 1989). The third event of metamorphism  $M_3$  (post-MCT) was the retrograde metamorphism evidenced by alternation of garnet to biotite and biotite to chlorite along the rims of the garnet (Fig. 5f) during exhumation. Likewise, the Lesser Himalaya zone first experienced the burial regional metamorphism  $M_0$  (pre-MCT/eo-Himalayan) due to the overlying succession, evidenced by one set of foliations ( $S_0=S_1$ ) below the MCT (Figs. 4a,b). It is followed by Barrovian type garnet grade inverted metamorphism  $M_1$  (neo-Metamorphism/ syn-MCT) as the present study area belongs to garnet zone indicating the increase in metamorphic grade towards the younger sequences instead of decreasing. Stratigraphically, the biotite zone belongs to older sequences that lie in the lower section whereas garnet zone in the upper section (Pokhrel, 2015). It is followed by late phase post-MCT retrogressive metamorphism evidenced by the alternation of garnet into biotite along the rim of garnet grain (Fig. 6a,b).

**Table 1: Lithostratigraphy correlation of the present study with the other section of the Higher Himalaya.**

Lombard (1958)		Bordet et al. (1972)		Le Fort, (1975); Colchen et al. (1986)		Hayashi et al. (1984)		Arita et. al. (1984)		Present study		Age Le Fort (1975)
Tibetan Slab	Quartzite-Mica Schist	Tibetan Slab	Kyanite (Sillimanite-Gneiss)	Tibetan Slab	Formation I	Himalayan gneiss group	Garnet Biotite Gneiss	Himalayan Gneiss	Mylonitized Gneiss	Banded Gneiss II	Pre-cambrian	
										Kyanite-Garnet Gneiss		
										Banded Gneiss I		
										Banded Gneiss and Quartzites		
										Kyanite Gneiss		

**Table 2: Lithostratigraphy correlation of the present study with the other section of the Lesser Himalaya.**

Hashimoto et al. (1973)		Stocklin (1980)		Sakai (1985)		Dhital et al. (2002)		Present Study	Age (Stöcklin and Bhattarai, 1977)
Midland Metasedimentary Group	Arenaceous Succession	Upper Nawakot Group	Benighat Slate	Kaligandaki Super Group	Ramdighat	Upper Nawakot Group	Benighat	Laminated Quartzite and Garnet Schist	Mesoproterozoic(?)
								Graphitic Schist	
	Argillaceous Succession	Lower Nawakot Group	Dhading Dolomite		SaidiKhola Khoraidi Chappani	Dhading Dolomite	Metacarbonates	Mesoproterozoic (?)	
			Nourpul Formation		Virkot	Lower Nawakot Group	Nourpul Formation	White Quartzites and Schist	Mesoproterozoic (?)
		Dandagaon Phyllite	Heklang	Nayagaon Formation	Pelitic Schist	Paleoproterozoic			

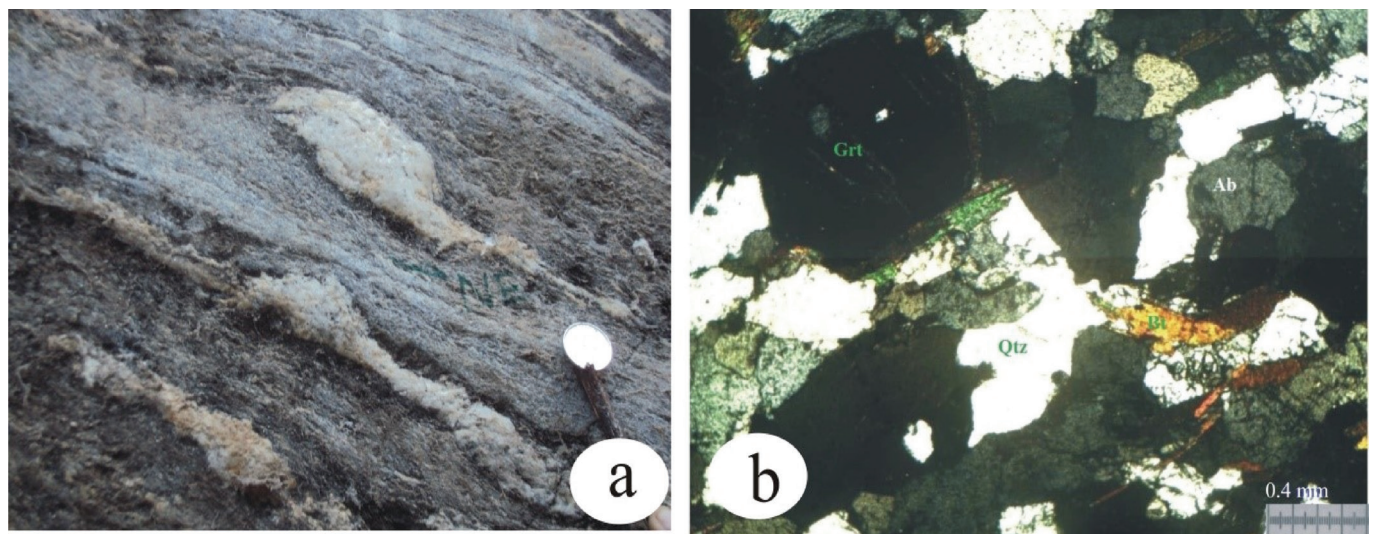


**Fig. 6: (a) Photograph showing top to the south of shear in boudin in Higher Himalaya, (b) Photomicrograph showing the porphyritic garnet alteration of garnet into biotite along the rims of garnet in in schist of White Laminated Quartzite and Garnet Schist of Lesser Himalaya. Abbreviations of minerals in alphabetic orders: Act: Actinolite, Bt: Biotite, Cl: Chlorite, Dol: Dolomite, Grt: Garnet, Hbl: Hornblende, Ky: Kyanite, Or: Orthoclase, Tre: Tremolite.**

## DISCUSSION

### Lithostratigraphy

The study area comprises the litho-units of the Lesser Himalaya in the south and Higher Himalaya in the north, separated by the MCT (Fig. 2, 3). The MCT is observed based on the distinct change in lithology and metamorphic grade following Le Fort (1974) and is equivalent to the MCT II (Arita, 1983), Upper MCT (Poudel and Arita, 2002). The litho-units of the Higher Himalaya of present study are correlated to the Formation I of Le Fort (1975) (Table 1). Formation I of Le Fort (1975) begins with kyanite garnet banded gneiss of pelitic to arenaceous composition with segregated quartz and the kyanite-garnet bearing banded gneiss occurrence in the uppermost part of the succession. It is similar to the present litho units that consist of the thick succession of kyanite-garnet bearing paragneiss in its lowermost part. It is followed by two mica rich gneiss, quartzites and banded gneiss with abundance segregated quartz lenses with subordinate coarsely crystalline quartzite. And, the alternation of light quartz rich to dark mica-rich banded gneiss and white to dark grey kyanite-garnet paragneiss followed by biotite poor banded gneiss and migmatites in the uppermost part of the study area. However, sillimanite was not observed in present study.

From lower to upper section, the present litho-units of the Lesser Himalaya zone represent five litho units as Pelitic Schist, White Quartzite and Schist, Metacarbonates, Graphitic Schist and White Quartzite and Garnet Schist (Fig. 2). Based on the origin, distinct lithological characteristics, metamorphic facies and structural similarities, these lithological successions can be correlated with to the Nawakot Complex of Lesser Himalaya (Larson and Godin, 2009; Stocklin, 1980: Table 2), the Lower Greater Himalaya Sequences of Greater Himalaya Sequence (Parson et al., 2016), Main Central Thrust Zone (Arita et al., 1982), Upper Midland Formation (Colchen et al., 1980). However, the present discussion follows the Nawakot Complex of the Lesser Himalaya (Larson and Godin, 2009; Stocklin, 1980), (Table 3). Accordingly, the formations of the present study are correlated with the Dandagaon Phyllite, Nourpul Formation, Dhading Dolomite and Benighat Slate from bottom to top respectively (Table 2). The Dandagaon Phyllite is characterised by dark blue-green argillaceous to finely quartzite-phyllites (Stocklin, 1980). However, it is represented by the light silky grey phyllite and biotite chlorite schist of the Pelitic Schist in present study. The biotite chlorite schist is metamorphosed form of the argillaceous phyllite. White Quartzite and Schist represents the Nourpul Formation that consists of thick succession of coarse grained, banded micaceous quartzites at the base as Purebesi Quartzite, followed by the dominance of light grey pelitic schist to psammitic schist at middle to the thin alteration of quartzites and light to dark grey schist to the top. The grey-green to blue-grey phyllite of Nourpul formation is metamorphosed to the schist (Stocklin,

1980). The Dhading Dolomite as Metacarbonates in present study is characterized by the massive, thickly bedded siliceous dolomitic marble with thin bands of calcareous quartzite. The siliceous dolomite and the lenticular chert bands have been metamorphosed to the siliceous dolomitic marble and calcareous quartzites respectively. However, the stromatolites are not preserved due the metamorphism. The Benighat Slate as Graphitic Schist consists of coaly black graphitic schist, dark grey phyllite and light to dark grey pelitic schist and psammitic schist followed by the calcareous quartzites and calcareous schist. The dark bluish grey to black slates and phyllites of the Benighat Slate is metamorphosed to the graphitic schist, pelitic and psammitic schist. The Jhiku carbonate bed with varying lithotype as siliceous dolomite interbedded with black slates has been metamorphosed to calcareous quartzites and calcareous schist. The Jhiku carbonate is followed by the White Quartzite and Garnet Schist characterized by micaceous white quartzites and deformed garnet schist which is also the part of the Benighat Formation (Pokhrel, 2015). The study area belongs to the northern limb of Gorkha-Pokhara anticlinorium and approaches to the MCT (Vanne and Hodges., 1996). So, the grade of metamorphism of the litho-units of the Lesser Himalaya are higher in this section than that of the lithostratigraphy mentioned in central Nepal by Stocklin (1980).

### Metamorphic zonation and metamorphic facies

Two metamorphic zones are identified as garnet zone and kyanite zone, separated by the MCT (Fig. 2). The kyanite isograd was mapped with the first appearance of the kyanite exposed around Naiche, Badalbisaune, Probi and Bahundanda. And it coincides with the MCT which is similar to mapping of it in various section of Nepal Himalaya (Bordet, 1961; Colchen et al., 1986; Johnson et al., 2001; Le Fort, 1975) and the MCT II along Modi Khola section (Arita, 1983). The present study concludes that the metamorphic grade intensity is increasing towards the north like in the adjacent region (Hodges et al., 1996; Larson and Godin, 2009; Le Fort, 1975; Paudel and Arita, 2002).

The chlorite grade green-schist facies to garnet grade upper green-schist-amphibolite facies in the upper section of the Lesser Himalaya and kyanite to sillimanite metamorphic grade facies (amphibolite to granulite facies) have been recorded in the Higher Himalaya (Hodges et al., 1996; Larson and Godin, 2009). However, the study area is limited to certain part of Nawakot Complex of the Lesser Himalaya which is equivalent to Upper MCT Zone or Midland Formation (Arita, 1983; Le Fort, 1975; Stocklin, 1980) and Formation I of the Higher Himalaya (Le Fort, 1975). It is characterized by kyanite grade Amphibolite Facies. In present study, the Lesser Himalaya rock succession characterized by the mineral assemblages as  $Grt+Bt+Ms+Chl+Pl+Qtz$  belongs to Epidote-Amphibolite Facies and Higher Himalaya rock succession characterized by the mineral assemblages as  $Ky+Grt+Ms+Bt+Pl$  belongs to Amphibolite Facies (Table 3).

**Table 3: Metamorphic zonation and metamorphic facies of study area.**

Tectonic Division	Present Study	Metamorphic Zone	Mineral Assemblages		Metamorphic Facies
			Pelitic/Psammatic Rocks	Calcareous Rock	
Higher Himalaya	Banded Gneiss II	Kyanite Zone	Kyanite, Garnet, Biotite, Muscovite, Quartz, Albite, Orthoclase, Plagioclase		Amphibolite Facies
	Kyanite-Garnet Gneiss				
	Banded Gneiss I				
	Banded Gneiss and Quartzites				
	Kyanite Gneiss				
Lesser Himalaya	Laminated White Quartzite and Garnet Schist	Garnet Zone	Garnet, Biotite, Muscovite, Quartz, Chlorite, Plagioclase	Calcite, Dolomite, Quartz, Muscovite, Plagioclase, Biotite, Tremolite, Actinolite	Epidote-Amphibolite Facies
	Graphitic Schist				
	Metacarbonates				
	White Quartzite and Schist				
	Pelitic Schist				

### ***Poly-phase metamorphism***

The stages of metamorphic events are studied in the Higher and Lesser Himalaya by various researchers in Central Nepal Himalaya (Le Fort 1975; Le Fort et al. 1986; Caby et al., 1983; Paudel and Arita, 1983; Hodges et al., 1996; Vannay and Hodges, 1996; Paudel and Arita, 2000; Larson and Godin, 2009; Martin et al., 2009; Paudel, 2011). They have also mentioned that the increase in metamorphic grade structurally towards upper section from chlorite grade-lower green schist facies to garnet grade-upper green schist facies in the Lesser Himalaya resulting the inverse metamorphism and medium temperature/ high pressure kyanite grade Barrovian type prograde metamorphism followed by the high temperature/ low pressure sillimanite grade metamorphism in the Higher Himalaya which is similar to the present study area. Likewise, the metamorphic grade increases from south to north showing multistage or polyphase of metamorphic events in the Khudital area (Fig. 2). However, sillimanite occurrence is not observed in this section.

In the present study, three metamorphic events are recognized in the Higher Himalaya and Lesser Himalaya. The kyanite rich medium temperature/ high pressure amphibolite facies barrovian type prograde metamorphism  $M_1$  (eo-Himalayan/ pre-MCT) is followed by metamorphism  $M_2$  (neo-Himalayan/ syn-MCT) indicated by the spiral quartz inclusion within the garnet, top to south sense of indicator in asymmetric boudin and NNE sense of shearing indicated by the lineated kyanite and mica minerals. It is due to the shearing and thrusting along the MCT during upliftment (Stäubli, 1989). The  $M_2$  is over

printed by late phase post- MCT retrograde metamorphism  $M_3$  with alteration of garnet into biotite along the rims of garnet during exhumation (Paudel and Arita, 2000). Similarly, the Lesser Himalaya first experienced the burial regional prograde metamorphism  $M_1$  (pre-MCT/ eo-Himalayan), evidenced by one set of foliations ( $S_0=S_1$ ) below the MCT (Pandey and Paudyal, 2020).  $M_1$  is followed by garnet grade prograde inverted metamorphism  $M_2$  (neo-Metamorphism/ syn-MCT) as present study area of the Lesser Himalaya belongs to northern limb of the Gorkha-Pokhara anticlinorium approaching the MCT and characterized by garnet zone indicating the increase in metamorphic grade towards the younger sequences instead of decreasing (Le Fort et al., 1986; Vannay and Hodges, 1996; Paudel and Arita, 2002). Stratigraphically, the biotite zone belongs to older sequences than garnet zone in the upper section (Pokhrel, 2015). Further  $M_2$  was overprinted by the late phase post-MCT retrogressive metamorphism ( $M_3$ ) with replacement of garnet by biotite and chlorite (Paudel and Arita, 2002; Rai et al., 2005).

### ***Pressure and temperature conditions***

The present study lacks the P-T result. However, the study regarding P-T condition has been carried out in adjacent region of the Central Nepal along the Kaligandaki River (Le Fort et al., 1986; Vannay and Hodges, 1996), Langtang region (Macfarlane, 1995), Gosainkund Crystalline Nappe in Kathmandu region (Rai et al., 1998), Darondi River (Kohn et al., 2001), Modi Khola (Martin et al., 2009). Based on Ga-Bt geothermometry observation by Le Fort et al. (1986) and

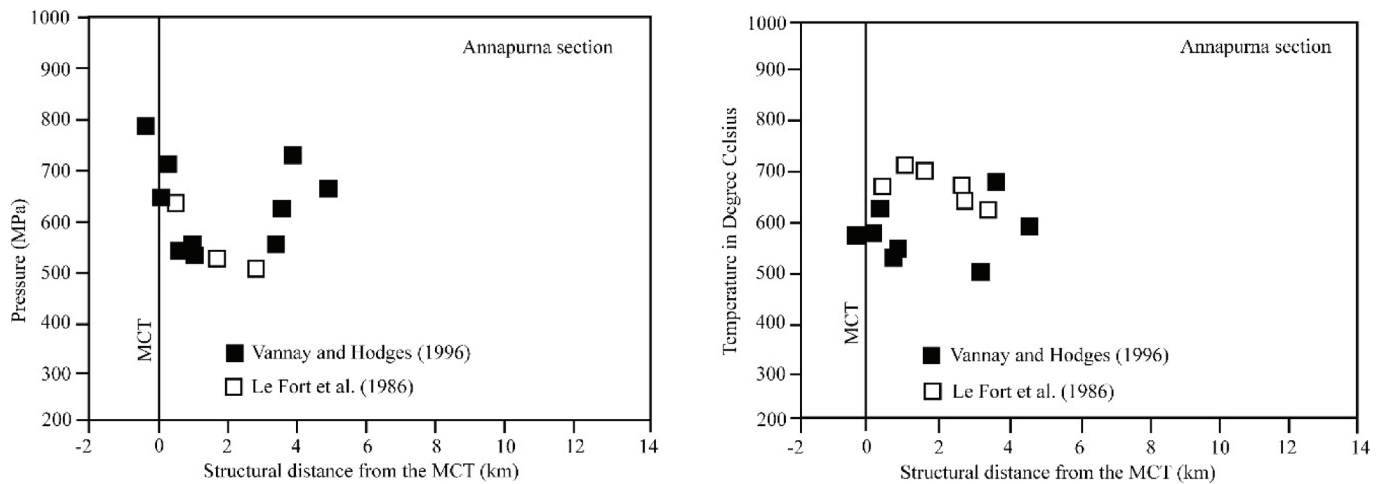


Fig. 7: Pressure-temperature estimations plotted as a function of structural distance (Le Fort et al. 1986, Vannay and Hodges, 1996).

Vannay and Hodges (1996), the temperature range between 530 °C to 720 °C and pressure from 550 to 900 MPa (Fig. 7) above the MCT i.e., in the rocks of the Higher Himalayan. The 530 °C is supposed to be the resulting temperature of the rim pairs of same geothermometry (Vannay and Hodges, 1996). Rai et al. (1998), estimated the temperature and pressure condition of the Higher Himalaya range as 540 °C - 615 °C and 405-790 MPa of the Gosainkund Crystalline Nappe and the Lesser Himalaya as 530 °C and 745 Mpa of the Kathmandu Region, based on Thermocalc calibration method. Accordingly, the estimated pressure when plotted across the structural distance to the MCT, gradually decreases towards upper section (Fig. 7). However, from west to east the pressure increases from 650 ± 30 MPa, whereas the temperature increases from 450 ± 65 °C to 605 ± 100 °C (Pecher, 1989). Also, Khon et al. (2001) observed a temperature and pressure values as 625 °C - 725 °C and 7-11 kbar based on thermometry along the Dorandi River section. The P-T-t path shows initially an increment in both temperature and pressure which was due to loading, followed by decrease in both temperature and pressure during exhumation (Harrison et al., 1998; Kohn et al., 2001). In the Lesser Himalaya, based on thermobarometry, Kohn et al. (2001) reported the increase in pressure and temperature condition from 525 °C and 5-6 Kbar to 625 °C and 11-1 Kbar structurally upward from base towards the Higher Himalayan along the Dorandi River. However, inverted metamorphism with the inversion of isograds are common fact along the MCT zone (Le Fort, 1975; Hodges et al., 1988). The Monazite Th-Pb age data indicates the initial metamorphism of the Lesser Himalaya rocks was at or before 20 Ma and later metamorphic overprinting or re-quillibration to 8 Ma, after which rapid movement along the MCT decreases the pressure and temperature resulting cooling of prior heated rocks (Kohn et al., 2001). The observation of the P-T result from the different section of the Central Nepal Himalaya indicates the different metamorphic event in different time. In the present study, based on the stratigraphic position and lithological

correlation, P-T condition of the Higher Himalaya along the Marsyangdi Khola section should range between 530 °C to 720 °C and 550-900 Mpa. Accordingly, the kyanite grade prograde metamorphism as  $M_1$  (pre-MCT/ Eo-Himalayan) should be the result of the initial increase in temperature more than 700 °C and with pressure range 7-15 Kbar due to crustal thickening in Middle Eocene to Oligocene (Vannay and Hodges, 1996; Kohn et al., 2001). Later, the decrease in temperature around 540 ± 30 °C and 650 ± 30 Mpa is due to overthrusting of the Higher Himalaya rocks over the Lesser Himalaya resulting  $M_2$  (syn-MCT/ neo-Metamorphism) in Oligocene to Early Miocene followed by  $M_3$  (post-MCT retrogressive metamorphism) during exhumation in Early Miocene to Middle Miocene. Similarly, the P-T condition of the Lesser Himalaya in this section should range between 523 °C to 625 °C and 5.6 Kbar to 11 Kbar. Here, the initial increase in P-T condition should be during  $M_1$  (burial prograde regional metamorphism) in early Paleozoic (Paudel and Arita, 2000), followed by the  $M_2$  (syn-MCT/ neo-Metamorphism), garnet grade prograde inverted metamorphism) during Early Miocene (Harrison et al., 1995) to  $M_3$  (post-MCT retrogressive metamorphism) during Middle Miocene (Vannay and Hodges., 1996).

## CONCLUSIONS

The Khudi Tal area along the Marsyangdi valley consists of the lithological units of the Lesser Himalaya and the Higher Himalaya, separated by the MCT. The lithological succession of Higher Himalaya comprises the Kyanite Gneiss, Banded Gneiss and Quartzites, Banded Gneiss I, Kyanite-Garnet Gneiss and Banded Gneiss II from bottom to top, respectively. Similarly, the Lesser Himalaya is characterized by the Pelitic Schist, white Quartzite and Schist, Meta Carbonates, Graphitic Schist and Laminated Quartzite and Garnet Schist from bottom to top, respectively.

With increasing the intensity of the metamorphism towards north, structurally upper section, the Higher Himalaya in present study, belongs to amphibolite facies with the mineral

assemblages as Ky+Grt+Qtz+Ms+Bt+Pl. The amphibolite facies metamorphic rocks are kyanite garnet gneiss to banded gneiss. The Lesser Himalaya belongs to epidote-amphibolite facies with mineral assemblages as Grt+Bt+Ms+Chl+Pl+Qtz in pelitic rocks, Bt+Ms+Chl+Pl+Qtz in psammatic rocks and Cal/Dol+Qtz+Pl+Bt+Ms in calcareous rocks. The epidote-amphibolite facies metamorphic rocks are pelitic to psammatic schist, quartzites, dolomitic to siliceous marble and garnet-schist. Two metamorphic zones are recorded as the garnet zone in the south and kyanite zone in the north, separated by kyanite isograd which coincides with MCT. The metamorphic events;  $M_1$ ,  $M_2$  and  $M_3$  represents the eo-Himalayan/ pre-tectonic prograde metamorphism to syn-MCT to post-MCT late phase retrogressive metamorphism in the Higher Himalaya. The Lesser Himalaya experiences the metamorphic events  $M_1$  as pre-MCT/ eo-Himalayan burial regional metamorphism followed by  $M_2$  as barrovian type prograde inverted syn-MCT/ neo-Metamorphism to late phase post-MCT retrogressive metamorphism  $M_3$ .

#### ACKNOWLEDGEMENT

The authors are thankful to Prof. Dr. Khum Narayan Paudyal and Asst. Prof. Dr. Kabi Raj Paudyal for their guidance during research. The authors are also thanks to Subash Acharya for the help in data collection and analysis.

#### REFERENCES

- Arita, K., 1983, Origin of the inverted metamorphism of the Lower Himalayas, Central Nepal. *Tectonophysics*, 95(1-2), pp. 43–60.
- Arita, K., 1984, Geology and structure of the Jajarkot–Piuthan area, Central Nepal. *Jour. Nepal Geol. Soc.*, v. 4, pp. 5–28.
- Arita, K., Shiraishi, K., and Hayashi, D., 1984, Geology of western Nepal and a comparison with Kumaun India. *Journal of the Faculty of Science, Hokkaido University (Japan)*, Series 4, Geology and mineralogy, 21(1), pp. 1–20.
- Avouac, J. P., 2003, Mountain building, erosion and the seismic cycle in the Nepal Himalaya. *Advances in Geophysics*, 46, pp. 1–80.
- Bollinger, L., Henry, P., and Avouac, J. P., 2006, Mountain building in the Nepal Himalaya: Thermal and kinematic model. *Earth and Planetary Science Letters*, 244(1), pp. 58–71.
- Bordet, P., Colchen, M., and Le Fort, P., 1972, Some features of the geology of the Annapurna Range, Nepal Himalaya. *Himalayan Geology*, 2, pp. 537–563.
- Caby, R., Pêcher, A., and Le Fort, P., 1983, Le grand Chevauchement central himalayen: nouvelles données sur le métamorphisme inverse à la base de la Dalle du Tibet. *Revue de Géographie physique et de Géologie Dynamique*, Paris, 24, pp. 89–100.
- Catlos, E. J., Harrison, T. M., Kohn, M. J., Grove, M., Ryerson, F. J., Manning, C. E., and Upreti, B. N., 2001, Geochronologic and thermobarometric constraints on the evolution of the Main Central Thrust, central Nepal Himalaya. *Journal of Geophysical Research: Solid Earth*, 106(B8), pp. 16177–16204.
- Colchen, M., Fort, P., and Pêcher, A., 1980, Carte Géologique Annapurna–Manaslu–Ganesh, Himalaya du Nepal. Echelle 1:200,000. Centre National de la Recherche Scientifique, Paris.
- Colchen, M., Le Fort, P., and Pêcher, A., 1986, Recherches géologiques dans l’Himalaya du Népal. Annapurna–Manaslu–Ganesh, Paris, Centre de Recherches Paris (in French and English), 136 p.
- Corrie, S. L. and Kohn, M. J., 2011, Metamorphic history of the central Himalaya, Annapurna region, Nepal, and implications for tectonic models. *Geological Society of America Bulletin*, 123(9-10), pp. 1863–1879.
- Dhital, M. R., 2015, Geology of the Nepal Himalaya: Regional perspective of the classic collided Orogen. Springer Cham Heidelberg, New York, Dordrecht London, 498 p.
- Dhital, M. R., Thapa, P. B., and Ando, H., 2002, Geology of the inner Lesser Himalaya between Kusma and Syangja in western Nepal. *Bulletin Dept. Geol.*, 9, pp. 1–60.
- Ehlers, E. G. and Blatt, H., 1982, Petrology, Igneous, Sedimentary and Metamorphic. W. H. Freeman and Company, San Francisco, 732 p.
- Gansser, A., 1964, Geology of the Himalaya. Interscience Publishers, London, 289 p.
- Gehrels, G., DeCelles, P., Martin, A., Ojha, T. P., Pinhassi, G., and Upreti, B. N., 2003, Initiation of the Himalayan orogen as an early Paleozoic thin-skinned thrust belt. *Gsatoday*, 13(9), pp. 4–9.
- Godard, V., Bourlès, D. L., Spinabella, F., Burbank, D. W., Bookhagen, B., Fisher, G. B., Moulin, A., and Léanni, L., 2014, Dominance of tectonics over climate in Himalayan denudation. *Geology*, 42(3), pp. 243–246.
- Harrison, T. M., Grove, M., Lovera, O. M., and Catlos, E. J., 1998, A model for the origin of Himalayan anatexis and inverted metamorphism. *Jour. Geophys. Res.: Solid Earth*, 103(B11), pp. 27017–27032.
- Harrison, T. M., Ryerson, F. J., Le Fort, P., Yin, A., Lovera, O. M., and Catlos, E. J., 1997, A late Miocene–Pliocene origin for the central Himalayan inverted metamorphism. *Earth and Planetary Science Letters* 146(1-2), pp. 1–7.
- Hashimoto, S., Ohta, Y., and Akiba, C., 1973, Geology of Nepal Himalayas. Saikon, Japan, pp. 1–286.
- Hayashi, D., Fujii, Y., Yoneshiro, T., and Kizaki, K., 1984, Observations on the geology of the Karnali region, west Nepal. *Jour. Nepal Geol. Soc.*, v. 4, pp. 29–40.
- Hodges, K., Hubbard, M. S., and Silverberg, D. S., 1988, Metamorphic constraints on the thermal evolution of the central Himalayan Orogen. *Philosophical Transactions of the Royal Society of London*, A326(1589), pp. 257–280.
- Hodges, K., Parrish, R. R., and Searle, M. P., 1996, Tectonic evolution of the central Annapurna Range, Nepalese Himalayas. *Tectonics*, 15, pp. 1264–1291.
- Hubbard, M. S. and Harrison, T. M., 1989,  $^{40}\text{Ar}/^{39}\text{Ar}$  age constraints on deformation and metamorphism in the Main Central Thrust zone and Tibetan Slab, eastern Nepal Himalaya. *Tectonics*, 8(4), pp. 865–880.
- Johnson, M. R. W., Oliver, G. J. H., Parrish, R. R., and Johnson, S. P., 2001, Synthrusting metamorphism, cooling, and erosion of the Himalayan Kathmandu Complex, Nepal. *Tectonics*, 20(3), pp. 394–415.
- Khanal, S. and Robinson, D. M., 2013, Upper crustal shortening and forward modeling of the Himalayan thrust belt along the Budhi-

- Gandaki River, central Nepal. *International Journal of Earth Sciences*, 102(7), pp. 1871–1891.
- Kohn, M. J., 2008, P–T–t data from central Nepal support critical taper and repudiate large-scale channel flow of the Greater Himalayan Sequence. *Geol. Soc. America Bull.*, 120(3–4), pp. 1–15.
- Kohn, M. J., Catlos, E. J., Ryerson, F. J., and Harrison, T. M., 2001, Pressure–temperature–time path discontinuity in the Main Central thrust zone, central Nepal. *Geology*, 29(7), pp. 571–574.
- Kretz, R., 1983, Symbols for rock-forming minerals. *American mineralogist*, 68(1–2), pp. 277–279.
- Larson, K. P. and Godin, L., 2009, Kinematics of the greater Himalayan sequence, Dhaulagiri Himal: implications for the structural framework of central Nepal. *Journal of the Geological Society*, 166, pp. 25–43.
- Le Fort, P., 1975, Himalayas: the collided range. Present knowledge of the continental arc. *American Journal of Science*, 275(1), pp. 1–44.
- Le Fort, P., 1986, Metamorphism and magmatism during the Himalayan collision. Geological Society, London, Special Publications, 19(1), pp. 159–172.
- Lombard, A., 1958, Un itinéraire géologique dans l’Est du Népal (Massif du Mont Everest). *Mémoires de la Société Helvétique des Sciences Naturelles*, 82, pp. 1–107.
- Macfarlane, A. M., 1995, An evaluation of the inverted metamorphic gradient at Langtang National Park, central Nepal Himalaya. *Journal of metamorphic Geology*, 13(5), pp. 595–612.
- Martin, A. J., DeCelles, P. G., Gehrels, G. E., Patchett, P. J. and Isachsen, C., 2005, Isotopic and structural constraints on the location of the Main Central thrust in the Annapurna Range, central Nepal Himalaya. *Geol. Soc. America Bull.*, 117(7), pp. 926–944.
- Molnar, P. and Tapponnier, P., 1975, Cenozoic tectonics of Asia: effects of a continental collision. *Science*, 189(4201), pp. 419–426.
- Nadin, E. S. and Martin, A. J., 2012, Apatite thermochronometry within a knickzone near the Higher Himalaya front, central Nepal: No resolvable fault motion in the past one million years. *Tectonics*, 31(2), pp. 1–11.
- Pandey, L. and Paudyal, K. R., 2020, Precise Location and Mapping of the Main Central Thrust Zone in Reference to Micro-Structures and Deformation along Khudi–Tal Area of Marsyangdi Valley. *Bull. Dept. Geol.*, 22, pp. 33–40.
- Parrish, R. and Hodges, V., 1996, Isotopic constraints on the age and provenance of the Lesser and Greater Himalayan sequences, Nepalese Himalaya. *Geol. Soc. America Bull.*, 108(7), pp. 904–911.
- Parsons, A. J., Law, R. D., Searle, M. P., Phillips, R. J., and Lloyd, G. E., 2016, Geology of the Dhaulagiri–Annapurna–Manaslu Himalaya, Western Region, Nepal. 1: 200,000. *Journal of Maps*, 12(1), pp. 100–110.
- Paudel, L., 2011, K–Ar Dating of White Mica from the Lesser Himalaya, Tansen–Pokhara Section, Central Nepal: Implications for the Timing of Metamorphism, Nepal. *Journal of Science and Technology*, 12, pp. 242–251.
- Paudel, L. P. and Arita, K., 2000, Tectonic and polymetamorphic history of the Lesser Himalaya in central Nepal. *Journal of Asian Earth Sciences*, 18, pp. 561–584.
- Paudyal, K. R. and Paudel, L. P., 2011, Geological setting and lithostratigraphy of the Lesser Himalaya in the Mugling–Banspani area, central Nepal. *Jour. Nepal Geol. Soc.*, v. 42, pp. 51–64.
- Pearson, O. N. and DeCelles, P. G., 2005, Structural geology and regional tectonic significance of the Ramgarh thrust, Himalayan fold–thrust belt of Nepal. *Tectonics*, 24(4), pp. 1–26.
- Pêcher, A., 1975, The Main Central Thrust of the Nepal Himalaya and the related metamorphism in the Modi Khola cross–section (Annapurna Range). *Himalayan Geology*, 5, pp. 115–132.
- Pêcher, A., 1977, Geology of the Nepal Himalaya: deformation and petrography in the Main Central Thrust zone. *Ecologie et Géologie de l’Himalaya, Colloques Internationaux du Centre National de la Recherche Scientifique, Paris*, 268, pp. 301–318.
- Pêcher, A., 1978, Déformations et métamorphisme associés à une zone de cisaillement. Exemple du grand Chevauchement Central Himalayen (MCT), transversale des Anapurnas et du Manaslu, Népal. PhD Thesis, Université Scientifique et Médicale de Grenoble (unpublished), 187 p.
- Pêcher, A., 1989, The metamorphism in the central Himalaya. *Journal of Metamorphic Geology*, 7(1), pp. 31–41.
- Pokhrel, P., 2015, Geological structure and landslide susceptibility analysis using the logistic regression method from Sundar Bajar to BesiShahar Area. Master Thesis, submitted to Central Department of Geology, Tribhuvan University (unpublished), 87 p.
- Rai, S. M., Upreti, B. N., and Sakai, H., 2001, Geology, structure and metamorphism of the Taplejung Window and frontal belt, Eastern Nepal. *Jour. Nepal Geol. Soc.*, v. 24, pp. 26–28.
- Rai, S. M., Upreti, B. N., Yoshida, M., Bhattarai, T. N., Ulak, P. D., Dahal, R. K., Dhakal, S., Gajurel, A. P., and Koirala, M. P., 2005, Geology of the Lesser and Higher Himalayan zones along the Kaligandaki Valley, central–west Nepal Himalaya. In *Proceeding of JICA Regional Seminar on National Disaster, Kathmandu, Nepal*, pp. 43–56.
- Sakai, H., 1985, Geology of the Kali Gandaki Supergroup of the Lesser Himalayas in Nepal. *Memoirs of the Faculty of Science, Kyushu University (Japan). Series D, Geology*, 25(3), pp. 337–397.
- Schelling, D. and Arita, K., 1991, Thrust tectonics, crustal shortening, and the structure of the far-eastern Nepal Himalaya. *Tectonics*, 10(5), pp. 851–862.
- Searle, M. P., 2010, Low–angle normal faults in the compressional Himalayan orogen; Evidence from the Annapurna–Dhaulagiri Himalaya, Nepal. *Geosphere*, 6, pp. 296–315.
- Searle, M. P. and Godin, L., 2003, The South Tibetan detachment and the Manasluleucogranite: A structural reinterpretation and restoration of the Annapurna–Manaslu Himalaya, Nepal. *The Journal of Geology*, 111(5), pp. 505–523.
- Searle, M. P., Law, R. D., Godin, L., Larson, K. P., Streule, M. J., Cottle, J. M., and Jessup M. J., 2008, Defining the Himalayan main central thrust in Nepal. *Journal of the Geological Society*, 165(2), pp. 523–534.
- Stäubli, A., 1989, Polyphase metamorphism and the development of the Main Central Thrust. *Journal of Metamorphic Geology*, 7(1), pp. 73–93.

- Stöcklin, J., 1980, Geology of Nepal in its regional frame. *Journal of the Geological Society of London*, 137(1), pp. 1–34.
- Stöcklin, J. and Bhattarai, K. D., 1977, Geology of the Kathmandu area and central Mahabharat range, Nepal Himalaya. Report of Department of Mines and Geology, Kathmandu, United Nation Development Program (unpublished), 86 p.
- Tapponnier, P., Peltzer, G., and Armijo, R., 1986, On the mechanics of the collision between India and Asia. *Geological Society of London*, 19(1), Special Publications, pp. 113–157.
- Valdiya, K. S., 1980, The two intracrustal boundary thrusts of the Himalaya. *Tectonophysics*, 66(4), pp. 323–348.
- Vannay, J. C. and Hodges, K. V., 1996, Tectonometamorphic evolution of the Himalayan metamorphic core between the Annapurna and Dhaulagiri, central Nepal. *Journal of Metamorphic Geology*, 14(5), pp. 635–656.
- Wobus, C., Heimsath, A., Whipple, K., and Hodges, K., 2005, Active out-of-sequence thrust faulting in the central Nepalese Himalaya. *Nature*, 434(7036), pp. 1008–1011.